

Correlations Between Climate Network and Relief Data

T. K. D. Peron¹, C. H. Comin¹, D. R. Amancio², L. da F. Costa¹, F. A. Rodrigues², and J. Kurths^{3,4,5}

¹São Carlos Institute of Physics, University of São Paulo, São Carlos, São Paulo, Brazil

²Institute of Mathematics and Computer Science, University of São Paulo, São Carlos, São Paulo, Brazil

³Potsdam Institute for Climate Impact Research (PIK), 14473 Potsdam, Germany

⁴Department of Physics, Humboldt University, 12489 Berlin, Germany

⁵Institute for Complex Systems and Mathematical Biology, University of Aberdeen, Aberdeen AB24 3UE, United Kingdom

Abstract. In the last few years, the scientific community has witnessed an ongoing trend of using ideas developed in the study of complex networks to analyze climate dynamics. This powerful combination, usually called climate networks, can be used to uncover non-trivial patterns of weather changes along the years. Here we investigate the temperature network of North America region and show that two network characteristics, namely degree and clustering, have markedly differences between the Eastern and Western regions. We show that such differences are a reflection of the presence of a large network community in the western side of the continent. Moreover, we provide evidence that this large community is a consequence of the peculiar characteristics of the western relief of North America.

1 Introduction

Complex networks are powerful tools for describing the structure and functioning of a wide range of natural, technological and social systems (da Fontoura Costa et al., 2011). Owing to the general framework that the network theory provides, a mathematical representation of such systems is straightforward, allowing not just the description of networked topologies, but also leading to a better comprehension of dynamical processes in systems whose elements are connected in a non-trivial fashion (Boccaletti et al., 2006). In the past few years, complex networks have also been applied in climate sciences, creating this way the new field of *climate networks* (Tsonis et al., 2006, 2008; Tsonis and Swanson, 2008; Donges et al., 2009a,b; Gozolchiani et al., 2008; Tsonis and Roebber, 2004; Yamasaki et al., 2008). According to this paradigm, climate networks are formed by nodes, corresponding to spatial grid points in a given global climate data. These nodes are connected by edges, which correspond to statistical similarities between times series of

given climate variables (e.g., temperature, relative humidity, precipitation) associated to each node in the network. Although this field is relative new in the network research, several results have been reported showing that network measurements can indeed give new important insights into climate dynamics (Tsonis et al., 2006, 2008; Tsonis and Swanson, 2008; Donges et al., 2009a,b; Gozolchiani et al., 2008; Tsonis and Roebber, 2004; Yamasaki et al., 2008; Rheinwalt et al., 2012; Mheen et al., 2013; Runge et al., 2014). For instance, by using degree centrality measurements of climate networks, researchers were capable of identifying highly connected nodes, which turned out to be related with the North Atlantic Oscillation. These results revealed that climate networks can exhibit small-world properties due to long-range edges (called teleconnections) connecting highly distant nodes (Tsonis et al., 2006, 2008). Moreover, the analysis of the teleconnections unveiled by this framework has also shed light on the study of extreme climate events, such as the El Niño-Southern Oscillations (ENSO) (Tsonis and Swanson, 2008; Gozolchiani et al., 2008). More specifically, by constructing climate networks of the surface temperature field during El Niño and La Niña periods, it was found that ENSO has a strong impact on the stability of climate systems, which is manifested as the decrease of the temperature predictability during El-Niño years. It is worth noting that the application of concepts from complex network theory in climate sciences has brought new insights that could not be unveiled by using classical methods of climatology and statistics. Recently, by using cross-correlation and mutual information to construct climate networks and analyzing the betweenness centrality field (node centrality measurement based on shortest path lengths (Costa et al., 2007)), researches found wave-like structures that are related to surface ocean currents, detecting this way a backbone of significantly increased matter and energy flow in the global surface air temperature field (Donges et al., 2009a,b). Furthermore,

71 the authors also showed that these results cannot be achieved
 72 by using methods derived from multivariate analysis, such
 73 as principal component analysis (PCA) and singular spec-
 74 trum analysis (SSA) (Donges et al., 2009a). In this work, we
 75 extend the analysis of climate networks investigating the in-
 76 fluence of altitudes of the grid points on centrality measure-
 77 ments of the networks generated through similarities in tem-
 78 perature time series measured at the surface level. The main
 79 motivation for including the altitudes on the network model
 80 is the assumption that the flow of matter and energy can be
 81 affected by topographical barriers, leading to anomalies in
 82 the correlations between the time series of climate variables.
 83 Therefore, in order to uncover these phenomena and quan-
 84 tify the influence of the relief on the network correlations,
 85 for each node v we associate its geographical altitude h_v with
 86 centrality measurements of the climate network, such as be-
 87 tweenness and clustering coefficient.

88 We constructed climate networks allowing the existence of
 89 long-range connections. By detecting communities in the cli-
 90 mate networks, we found clusters that correspond to groups
 91 of nodes embedded in geographical areas of similar relief
 92 properties. Moreover, it was also found that the correlation
 93 patterns between centrality measurements and relief proper-
 94 ties vary according to the considered network community.
 95 Finally we point out a possible effect of time series inter-
 96 polation generated by stations in the degree and clustering
 97 coefficient fields of the networks.

98 2 Materials and Methods

99 2.1 Dataset description

100 Throughout the analysis we used the following databases:

101 (i) Monthly land temperature records from the National
 102 Center for Environmental Prediction/National Center for At-
 103 mospheric Research NCEP/NCAR (Kistler et al., 2001; Fan
 104 and Van den Dool, 2008) obtained from January 1948 to Jan-
 105 uary 2011. The dataset consists of a regular spatio-temporal
 106 grid with 0.5° of latitude and longitude resolution. Each grid
 107 point i has a temperature time series $T_i(t)$ associated, con-
 108 taining the time evolution of the monthly mean temperature.
 109 A visualization of stations employed in the analysis that origi-
 110 nated the database is shown in Fig. 1 (data provided by the
 111 NOAA, 2013).

112 (ii) Relief dataset provided by National Geophysical Data
 113 Center (NGDC, 2009) and consisting of 1-arc minute reg-
 114 ular gridded area measuring land topography and ocean
 115 bathymetry.

116 2.2 Complex networks measurements

117 In order to seek for relationships between the climate and
 118 relief, we use network measurements related to centrality and
 119 symmetry of connections. The most simple of them, referred

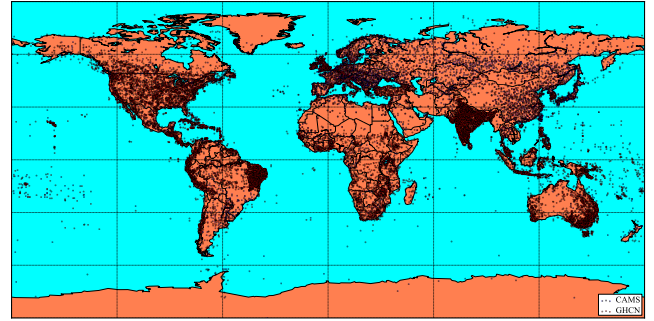


Fig. 1. Visualization of the stations used to interpolate the grid points in the temperature database.

to as node *degree*, is given by

$$k_i = \sum_{j=1}^N A_{ij}, \quad (1)$$

where $A_{ij} = 1$ if nodes i and j are connected and $A_{ij} = 0$ otherwise. The degree is a simple way to study the local importance of a node. Concerning climate networks, the degree can be used to quantify how many points of the studied region display a time series similar to a given point in the globe. In other words, nodes with large degrees are related to large regions of correlation.

The *clustering* coefficient of a node is the probability that two of its neighbors are also connected in the network, and is given by (da Fontoura Costa et al., 2011)

$$c_i = \frac{2\mathcal{T}(i)}{k_i(k_i - 1)}, \quad (2)$$

where $\mathcal{T}(i)$ is the number of triangles passing through i , or equivalently, the number of connections between neighbors of i . The clustering bears an interesting local information. If a given point of the globe is strongly correlated with two other points, the clustering quantifies how often these two points are also strongly correlated between themselves. The existence of regions taking low values of c_i suggests that the propagation of climate changes occurs in a streamlined fashion in those regions. Conversely, large clustering is related to a more diffusive propagation.

Another feature we study is *betweenness* centrality of a node. To define this measurement, consider the following notation. Let σ_{st} be the number of shortest paths from node s to node t (da Fontoura Costa et al., 2011). If $\sigma_{st}(i)$ is the number of such paths passing through node i , the betweenness centrality is given by (da Fontoura Costa et al., 2011)

$$b_i = \sum_{s \neq t \neq i} \frac{\sigma_{st}(i)}{\sigma_{st}}. \quad (3)$$

It gives information about global relationships in climate dynamics. It is of great importance in quantifying if a node is

commonly used as a route for long-range correlations in the network (Donges et al., 2009a).

A node can be central but still not communicate well with the rest of the network. For instance, a node that is connected to another with large degree can be regarded as being central in the network, but it has a strong dependence on its highly connected neighbor. The *accessibility* measurement quantifies the number of nodes effectively accessed after h steps, where the node accessed in the next step is chosen randomly. Formally, the accessibility is computed as

$$a_i = \frac{1}{N_i^h} \exp \left(- \sum_j P_{ij}^h \log P_{ij}^h \right), \quad (4)$$

where P_{ij}^h is the probability that a random walk starting at node i arrives at node j in h steps, N_i^h the number of reachable nodes in h steps from node i and $\exp(\cdot)$ is the exponential function (see, e.g., Viana et al., 2012 for a detailed explanation of this measurement).

Real-world networks often display a modular structure, i.e., the presence of communities (Fortunato, 2010). The modular structure of a given network can be quantified by the measurement known as *modularity*, which is given by (Newman, 2003)

$$Q = \frac{1}{2m} \sum_{ij} \left(A_{ij} - \frac{k_i k_j}{2m} \right) \delta(C_i, C_j), \quad (5)$$

where $m = 1/2 \sum A_{ij}$ is the total number of edges, C_i is the community to which node i belongs and δ is the Kronecker delta. Once the partitioning of the nodes into communities is done, the modularity Q basically calculates the fraction of edges that connects nodes of the same community subtracting the fraction of these edges that we would expect to find in a random graph with the same degree sequence. Thus, eq. 5 provides a significance test of the obtained network partitioning, which will be used to validate our results in the next sections.

Since the modularity Q quantifies how good a given partition is, many methods intended to uncover communities in networks are based on the optimization of this measurement. Different strategies for the modularity optimization have been adopted in the literature such as simulated annealing (Reichardt and Bornholdt, 2006; Guimera et al., 2004), greedy algorithms (Newman, 2004; Clauset et al., 2004) and extremal optimization (Duch and Arenas, 2005). Although these algorithms provide accurate results, most of them have great computational cost. For this reason, we adopt the method proposed in (Newman, 2006) to obtain the community structure of climate networks. This method consists in mapping the modularity optimization in terms of the spectrum of the so-called *modularity matrix* \mathbf{B} defined as

$$\mathbf{B} = \mathbf{A} - \frac{\mathbf{k}\mathbf{k}^T}{2m}, \quad (6)$$

where \mathbf{A} is the adjacency matrix, m is as defined before in eq. 5 and $\mathbf{k} = [k_1, \dots, k_N]^T$ the vector whose element k_i is the degree of the i -th node. The spectral optimization of the modularity Q has complexity of order $O(N^2 \log N)$, which turns out to be faster than, for instance, simulated annealing and extremal optimization approaches, besides providing more accurate results for large networks (Newman, 2006; Fortunato, 2010).

2.3 Climate networks

Because we are most interested in the topological characteristics of climate networks and its correlations with relief heights, we consider now only the connected subgraph whose nodes are located inside a continent. Note that we do not simply extract the subgraph over land discarding any edges which connects nodes on the ocean, rather we recalculate the threshold ϵ by taking into account only the nodes in the spatio-temporal grid which are over land.

Having the values of temperatures for each grid point in the dataset, a simple way to infer that two points have similar dynamical evolution is through the Pearson correlation coefficient between pairs of time series, which is given by

$$\rho_{ij} = \frac{\langle T_i T_j \rangle - \langle T_i \rangle \langle T_j \rangle}{\sqrt{(\langle T_i^2 \rangle - \langle T_i \rangle^2)(\langle T_j^2 \rangle - \langle T_j \rangle^2)}}, \quad (7)$$

where T_i is the time series associated to a point i in the spatio-temporal grid and $\langle X \rangle$ means the average of the variable X . Furthermore, we also remove the mean annual cycle in order to avoid seasonal effects in the time series. In this section, we describe the approach employed in our analysis.

We start with a fully connected network where each grid point is a node and two nodes are connected through an edge with an associated weight given by ρ_{ij} . The fully connected network can be studied by using weighted versions of the characteristics presented in section 2.2 (cf. Boccaletti et al., 2006 for a description of weighted measurements for graphs). Nevertheless, we are only interested in connections representing strong correlations. Hence, connections having a correlation smaller than a given threshold ϵ are discarded. This leads to a network defined by the adjacency matrix \mathbf{A} whose elements are given by $A_{ij} = \Theta(\rho_{ij} - \epsilon) - \delta_{ij}$, where $\Theta(\cdot)$ is the Heaviside function. The threshold ϵ should be chosen in order to keep the network edges that correspond to strong correlation between time series, thus eliminating the non-relevant ones (Tsonis et al., 2006; Tsonis and Swanson, 2008; Tsonis et al., 2008; Gozolchiani et al., 2008; Donges et al., 2009a). Therefore, for all networks analysed in this approach, the threshold ϵ was chosen so that only 5% of the connections are kept in the network. Without the constraint of only first-neighbours connections, it is reasonable to expect a much richer pattern of connectivity with, e.g., presence of communities in the network, i.e., clusters of nodes that are more connected inside these groups than external nodes to

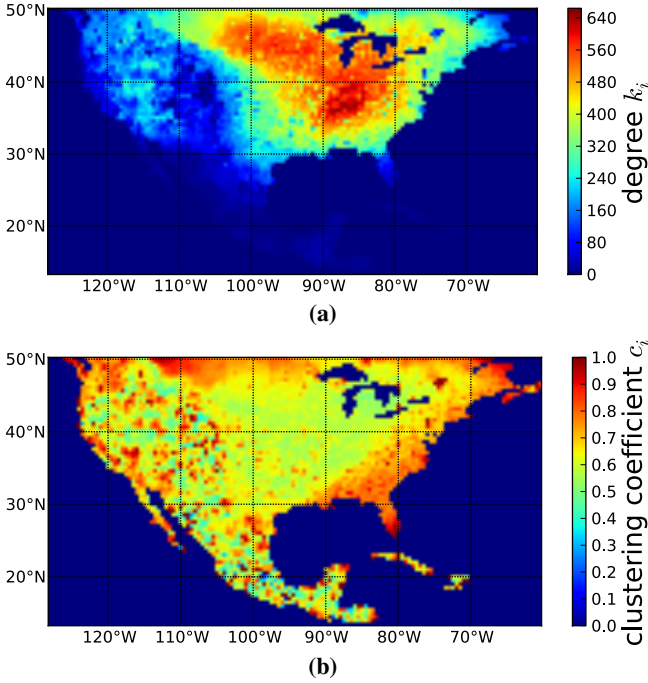


Fig. 2. (a) Degree k_i ; and (b) clustering coefficient c_i obtained from the network of temperature correlations.

249 the cluster. In the context of climate networks, the grouping
 250 of nodes into communities was shown to be related to dif-
 251 ferent climate patterns and to unveil different known climate
 252 zones (Tsonis et al., 2011).

253 3 Results

254 From reference (Fan and Van den Dool, 2008) we know that
 255 the land surface temperature database is constructed by inter-
 256 polating recorded time series from stations spread over the
 257 globe. In order to avoid interpolation effects, it is useful to
 258 analyze the spatial distribution of the stations that generate
 259 this database. Using data from (NGDC, 2009), in Fig. 1 we
 260 show the stations location used to record the monthly average
 261 temperature time series. As we can see, except the northeast
 262 region of Brazil, South American is sparsely covered by sta-
 263 tions, whereas North America and Europe are more densely
 264 covered. Therefore, in order to eliminate any doubts whether
 265 the observed patterns in the networks measurements are be-
 266 ing affected by the interpolation or not, we turn our analysis
 267 to regions with high density of stations, namely, the North
 268 America region.

269 Applying the methodology described in Section 2.3, we
 270 obtain the climate networks and extract the centrality mea-
 271 surements for the region with the values of longitude θ and
 272 latitude ϕ ranging in the intervals $-128^\circ \leq \theta \leq -60^\circ$ and
 273 $30^\circ \leq \phi \leq 70^\circ$, respectively. Our results are shown in Fig. 2.

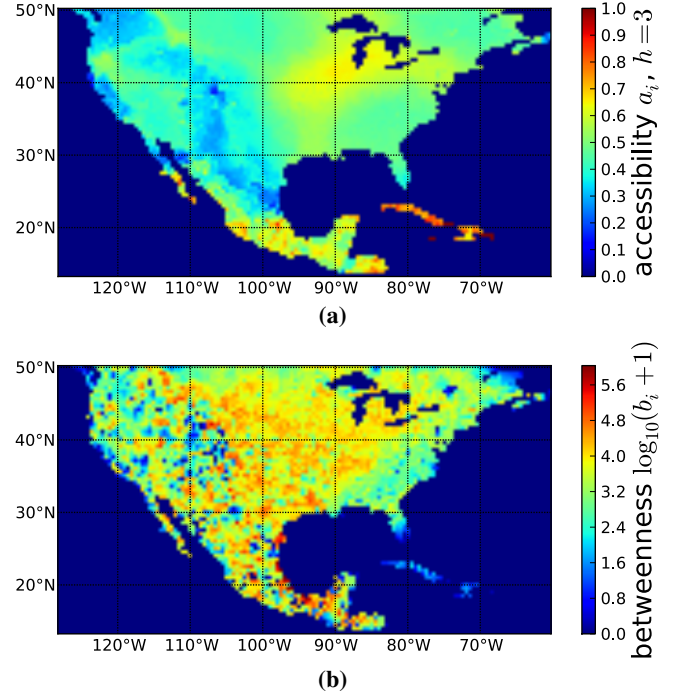


Fig. 3. (a) Betweenness centrality b_i ; and (b) accessibility a_i for $h = 3$ steps obtained from the network of temperature correlations.

275 As we can see in Fig. 1, the region has stations approximately
 276 uniformly distributed. Therefore, we can discard the hypothe-
 277 sis that the area with high values for the degree in Fig. 2(a)
 278 is due to interpolation effects. It is also interesting to note
 279 that in Fig. 2(b) there are two distinct patterns in the clus-
 tering coefficient field. While the eastern region has an al-
 most uniform distribution for c_i , the western region displays
 a more irregular distribution. The same pattern is also fol-
 lowed by the other centrality measurements. Figs. 3(a) and
 (b) shows the accessibility and betweenness centrality fields,
 respectively. Likewise, the patterns observed in the western
 and eastern regions differ significantly, especially for the ac-
 cessibility. It is important to note that, according to Figs. 2(a)
 and 3(b), the regions taking low values of degree and acces-
 sibility overlap significantly. This pattern cannot be interpreted
 in a straightforward fashion, as the relevant correlation be-
 tween degree and accessibility usually appears when the hier-
 archical definition of the degree is taken into account (Viana
 et al., 2012).

The topology of the climate network was further ana-
 lyzed by identifying the natural topological communities.
 The communities arising from the application of the eigen-
 vector strategy (see (Newman, 2006)) is shown in Fig. 4. A
 straightforward comparison of Figs. 2 and 4 reveals that the
 large community located at the western region corresponds to
 the nodes taking the lowest values of degree and accessibility

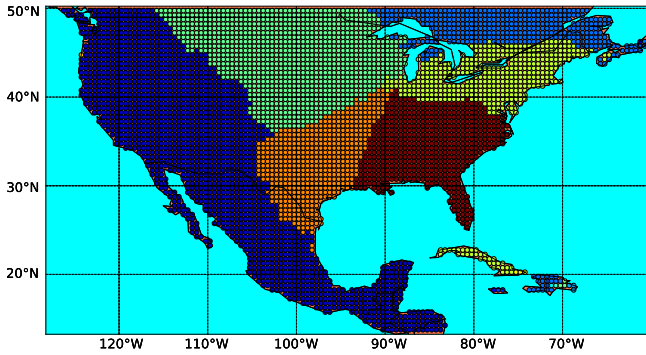


Fig. 4. Community structure for the network constructed with the grid points with θ and latitude ϕ in the intervals $-128^\circ \leq \theta \leq -60^\circ$ and $30^\circ \leq \phi \leq 70^\circ$ of the temperature database. Grid-points colored with the same color correspond to nodes belonging to the same network community.

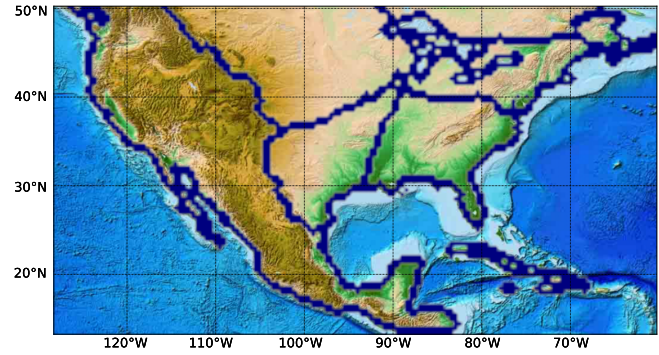


Fig. 5. Boundaries of the communities obtained from the climate networks. Note that the largest community coincides with a regular relief profile.

(see Figs. 2(a) and 3(a)). As for the clustering coefficient, it is irregularly distributed.

Fig. 5 displays the network communities and the relief structure. Remarkably, the variations in the largest community border in the west side of North America is followed by variations in the relief structure. Comparing Figs. 5 and 2, we notice that the contrast between the west and east region in the degree and clustering coefficient field is also observed in the relief structure. More specifically, the regions present very different patterns in the relief structure which is also revealed in the pattern of network measurements, suggesting that with our methodology we may be able to quantify the influence of the landscape in the climate network organization.

4 Conclusions

Despite being a recent field, climate networks have already been shown to provide valuable information about climate dynamics (Tsonis et al., 2006, 2008; Tsonis and Swanson, 2008; Donges et al., 2009a,b; Gozolchiani et al., 2008; Tsonis and Roebber, 2004; Yamasaki et al., 2008). In this study, we used the monthly land temperature records from NCEP/NCAR reanalysis to define correlations between stations, which are then transformed into network connections when they exceed a specified threshold. One important point raised during our investigation was the effect of the spatial distribution of stations on the resulting network. We found that data pertaining to the region in which $(-128^\circ, 30^\circ) \leq (\theta, \phi) \leq (-60^\circ, 70^\circ)$ should not suffer such effects, given its almost uniform distribution of stations. One important topic to be studied in the future is the specific effect of spatial heterogeneities in the sampled data on the formation of abnormal, but most likely predictable, structures in the network.

In this study, we showed that the North America, when modeled as a climate network, displays two regions with dis-

tinct topological properties. We have found that the eastern and western regions display striking differences of degree, accessibility and clustering coefficient, which may be explained by the presence of communities arising from the climate network. More specifically, the eastern side was found to be characterized by uniform values of centrality measurements. Conversely, the western side was mainly characterized by an heterogeneous distribution of measurements values. The relationship between climate and relief was analyzed in the relief dataset provided by NOAA jointly with the climate network data. Interestingly, we uncovered dynamics not detected by other traditional methods. The most important pattern arising from the analysis was the observation that the topological community of the climate network in the western region matched the region with peculiar relief structure, suggesting a strong influence of the relief on the climate dynamics.

Of paramount interest for future studies is to use other relevant climate variables (e.g., humidity, wind, pressure) to uncover additional relationships between relief and climate, using the ideas developed in the climate networks field, as well the boundary effects (Rheinwalt et al., 2012) of spatially embedded networks.

Acknowledgments

TKDP would like to acknowledge FAPESP (No. 2012/22160-7) and IRTG 1740. DRA is grateful for the financial support from FAPESP (grant number 2013/06717-4). FAR would like to acknowledge CNPq (No. 305940/2010-4), FAPESP (No. 2010/19440-2) and IRTG 1740 for the financial support given to this research. LdaFC is grateful for the financial support from CNPq, FAPESP and CAPES. JK would like to acknowledge IRTG 1740 (DFG and FAPESP) for the sponsorship provided.

367 **References**

- 368 Boccaletti, S., Latora, V., Moreno, Y., Chavez, M., and Hwang, 428
 369 D.: Complex networks: Structure and dynamics, *Physics reports*, 429
 370 424, 175–308, 2006. 430
- 371 Clauset, A., Newman, M. E., and Moore, C.: Finding community 431
 372 structure in very large networks, *Physical review E*, 70, 066 111, 432
 373 2004. 433
- 374 Costa, L., Rodrigues, F., Travesio, G., and Boas, P.: Characteriza- 434
 375 tion of complex networks: A survey of measurements, *Advances* 435
 376 *in Physics*, 56, 167–242, 2007. 436
- 377 da Fontoura Costa, L., Oliveira Jr, O., Travesio, G., Rodrigues, F., 437
 378 Boas, P., Antigueira, L., Viana, M., and Rocha, L.: Analyzing 438
 379 and modeling real-world phenomena with complex networks: a 439
 380 survey of applications, *Advances in Physics*, 60, 329–412, 2011. 440
- 381 Donges, J., Zou, Y., Marwan, N., and Kurths, J.: The backbone 441
 382 of the climate network, *EPL (Europhysics Letters)*, 87, 48 007, 442
 383 2009a. 443
- 384 Donges, J., Zou, Y., Marwan, N., and Kurths, J.: Complex networks 444
 385 in climate dynamics, *The European Physical Journal-Special* 445
 386 *Topics*, 174, 157–179, 2009b. 446
- 387 Duch, J. and Arenas, A.: Community detection in complex networks 447
 388 using extremal optimization, *Physical review E*, 72, 027 104, 448
 389 2005. 449
- 390 Fan, Y. and Van den Dool, H.: A global monthly land surface air 450
 391 temperature analysis for 1948–present, *Journal of Geophysical* 451
 392 *Research*, 113, D01 103, 2008. 452
- 393 Fortunato, S.: Community detection in graphs, *Physics Reports*, 453
 394 486, 75 – 174, 2010.
- 395 Gozolchiani, A., Yamasaki, K., Gazit, O., and Havlin, S.: Pattern 454
 396 of climate network blinking links follows El Nino events, *EPL* 455
 397 *(Europhysics Letters)*, 83, 28 005, 2008.
- 398 Guimera, R., Sales-Pardo, M., and Amaral, L. A. N.: Modularity 456
 399 from fluctuations in random graphs and complex networks, *Phys-* 457
 400 *ical Review E*, 70, 025 101, 2004.
- 401 Kistler, R., Kalnay, E., Collins, W., Saha, S., White, G., Woollen, J., 458
 402 Chelliah, M., Ebisuzaki, W., Kanamitsu, M., Kousky, V., et al.: 459
 403 The NCEP-NCAR 50-year reanalysis: Monthly means CD-ROM 460
 404 and documentation, *Bulletin-American Meteorological Society*, 461
 405 82, 247–268, 2001.
- 406 Mheen, M., Dijkstra, H. A., Gozolchiani, A., Toom, M., Feng, Q., 462
 407 Kurths, J., and Hernandez-Garcia, E.: Interaction network based 463
 408 early warning indicators for the Atlantic MOC collapse, *Geo-* 464
 409 *physical Research Letters*, 40, 2714–2719, 2013.
- 410 Newman, M. E.: Mixing patterns in networks, *Physical Review E*, 465
 411 67, 026 126, 2003.
- 412 Newman, M. E.: Fast algorithm for detecting community structure 466
 413 in networks, *Physical review E*, 69, 066 133, 2004.
- 414 Newman, M. E. J.: Finding community structure in networks using 467
 415 the eigenvectors of matrices, *Phys. Rev. E*, 74, 036 104, 2006.
- 416 NGDC (National Geophysical Data Center): Relief dataset, avail- 468
 417 able at; <http://www.ngdc.noaa.gov/mgg/global/global.html> (last 469
 418 access: 7 April 2014), 2009. 827, 830
- 419 NOAA (National Oceanic and Atmospheric Admin- 470
 420 istration): Datasets and variables, available at: 471
 421 <http://iridl.ldeo.columbia.edu/SOURCES/.NOAA/> (last ac- 472
 422 cess: 7 April 2014), 2013. 826
- 423 Reichardt, J. and Bornholdt, S.: Statistical mechanics of community 473
 424 detection, *Physical Review E*, 74, 016 110, 2006.
- 425 Rheinwalt, A., Marwan, N., Kurths, J., Werner, P., and Gersten- 474
 426 garbe, F.-W.: Boundary effects in network measures of spatially 475
 427 embedded networks, *EPL (Europhysics Letters)*, 100, 28 002, 476
 2012.
- 428 Runge, J., Petoukhov, V., and Kurths, J.: Quantifying the Strength 477
 429 and Delay of Climatic Interactions: The Ambiguities of Cross 478
 430 Correlation and a Novel Measure Based on Graphical Models., 479
 431 *Journal of Climate*, 27, 2014.
- 432 Tsonis, A. and Roebber, P.: The architecture of the climate network, 480
 433 *Physica A: Statistical Mechanics and its Applications*, 333, 497– 481
 434 504, 2004.
- 435 Tsonis, A. and Swanson, K.: Topology and predictability of El Nino 482
 436 and La Nina networks, *Physical Review Letters*, 100, 228 502, 483
 2008.
- 437 Tsonis, A., Swanson, K., and Roebber, P.: What do networks have 484
 438 to do with climate?, *Bulletin of the American Meteorological So-* 485
 439 *ciety*, 87, 585–596, 2006.
- 440 Tsonis, A., Swanson, K., and Wang, G.: On the role of atmospheric 486
 441 teleconnections in climate, *Journal of Climate*, 21, 2990–3001, 487
 2008.
- 442 Tsonis, A. A., Wang, G., Swanson, K. L., Rodrigues, F. A., and 488
 443 Costa, L. d. F.: Community structure and dynamics in climate 489
 444 networks, *Climate dynamics*, 37, 933–940, 2011.
- 445 Viana, M. P., Batista, J. a. L. B., and Costa, L. d. F.: Effective num- 490
 446 ber of accessed nodes in complex networks, *Phys. Rev. E*, 85, 491
 447 036 105, 2012.
- 448 Yamasaki, K., Gozolchiani, A., and Havlin, S.: Climate networks 492
 449 around the globe are significantly affected by El Nino, *Physical* 493
 450 *Review Letters*, 100, 228 501, 2008.